WARWICK
THE UNIVERSITY OF WARWICK

warwick.ac.uk/lib-publications

An advanced Lithium-ion battery optimal charging strategy based on a coupled thermoelectric model

Kailong Liu[a], Kang Li[a], Zhile Yang[a], Cheng Zhang[a], Jing Deng[a]

[a] *School of Electronics, Electrical Engineering and Computer Science, Queen's University Belfast, Belfast, BT9 5AH, United Kingdom (Email:{kliu02,k.li,zyang07,czhang07,j.deng}@qub.ac.uk).*

Abstract: Lithium-ion batteries are widely adopted as the power supplies for electric vehicles. A key but challenging issue is to achieve optimal battery charging, while taking into account of various constraints for safe, efficient and reliable operation. In this paper, a triple-objective function is first formulated for battery charging based on a coupled thermoelectric model. An advanced optimal charging strategy is then proposed to develop the optimal constant-current-constant-voltage (CCCV) charge current profile, which gives the best trade-off among three conflicting but important objectives for battery management. To be specific, a coupled thermoelectric battery model is first presented. Then, a specific triple-objective function consisting of three objectives, namely charging time, energy loss, and temperature rise (both the interior and surface), is proposed. Heuristic methods such as Teaching-learning-based-optimization (TLBO) and particle swarm optimization (PSO) are applied to optimize the triple-objective function, and their optimization performances are compared. The impacts of the weights for different terms in the objective function are then assessed. Experimental results show that the proposed optimal charging strategy is capable of offering desirable effective optimal charging current profiles and a proper trade-off among the conflicting objectives. Further, the proposed optimal charging strategy can be easily extended to other battery types.

Keywords: LiFePO$_4$ battery, Battery energy conversion, Coupled thermoelectric model, Teaching-learning-based-optimization

1. Introduction

To meet the unprecedented challenges on environmental protection and climate change, electric vehicles (EVs) and hybrid electric vehicles (HEVs) are developing rapidly in recent years [1]. Compared with conventional internal combustion engine (ICE) based vehicles, EVs are powered by batteries that may be charged from renewable power generated from the wind, solar or other forms of renewable sources [2]. Among all batteries types, Lithium-ion (Li-ion) batteries are preferable power supplies for EVs due to a number of favourable characteristics such as power density, less pollution, and long service life [3]. For Li-ion batteries, a proper battery charging strategy is essential in ensuring efficient and safe operations.

The charging strategy is a key issue in the battery management system (BMS) of EVs [4]. An optimal charging operation will protect batteries from damage, prolong the service life as well as improve the performance [5]. On the one hand, long charging time will inevitably affect the convenience of EV usage and limit its acceptance by customers [6]. However, too fast charging will lead to significant energy loss and battery performance degradation. It is therefore rational to consider the charging time as one of the key factors in designing the EVs charging control. Secondly, large energy loss implies low efficiency of energy conversion in battery charging, which needs to be addressed. Finally, both the battery surface and internal temperatures may exceed permissible level when it is charged with high current, and the overheating temperatures may intensify battery aging process and even cause explosion or fire in severe situations [7,8]. Thus, the battery charging time, energy loss, and temperature rises are important factors to be considered in designing the battery charging process.

Conventional methods used for battery charging can be divided into constant current (CC) strategy, constant voltage (CV) strategy and Mas Law strategy [9,10]. The constant current strategy simply uses a small constant current to charge battery along the whole process to avoid the steep rise in both the battery voltage and temperature. However, it is difficult to achieve a proper current rate to balance the battery charging time and the desired capacity. Another simple charging strategy utilizes CV to avoid over-voltage. This strategy however requires a high current at the beginning of the charging process which can be quite harmful to the battery life. While the Mas Law strategy calculates the charge current based on the 'Mas Three Laws' principle [11,12] discovered by American scientist J. A. Mas in researching the maximum acceptable charge current. According to the Mas Three Laws, the charging receptivity is proportional to the square root of the discharging capacity and the logarithm of the discharging current. Further, the charging receptivity after several different discharging rates is equal to the total charging receptivity after each rate. It should be noted however that the Mas Law strategy is mainly used to develop pulse charging strategy for significantly improving the charging acceptance ability of lead-acid batteries rather than Li-ion batteries [13,14].

The constant-current-constant-voltage (CCCV) strategy, which integrates the CC strategy and CV strategy, has become the most popular strategy for Li-ion battery charging [15]. In this strategy, a CC is injected into battery first and the battery terminal voltage increases until the maximum safe threshold is reached. Then the battery starts to be charged at a CV until the battery capacity meets the target. Although the CCCV strategy is simple to apply, the open problem is to select an appropriate charging current at the CC stage. High current may cause large energy loss, and the temperature may exceed permissible levels especially in high power applications. On

the other hand, low charging current may prolong the battery charging time, affect the convenience of EV usage and limit its acceptance by customers. Therefore, it is vital to develop a better strategy based on CCCV to improve the overall charging performance and to guarantee the battery operation safety.

Various approaches have been proposed to improve the battery charging performance in the literature. Methods involving computational intelligence techniques such as neural networks [16], gray prediction [17], fuzzy control [14,18], and ant-colony algorithm [19] have been proposed to optimize the charging current profile. Jiang et al. [14] propose a constant-polarization-based fuzzy-control charging strategy to adapt charging current acceptance with battery state of charge (SOC) stages. The charging time can be significantly shortened without obvious temperature rise compared to standard CCCV. Although these intelligent approaches are based on criteria such as fast charging and extended energy capacity, it is relatively expensive to tune the parameters in these algorithms. Further, none of the aforementioned charging approaches consider the energy loss during the battery charging process.

Some other strategies consider the battery charging as an explicit optimization problem. Hu et al. [20] present a dual-objective optimal charging strategy for both lithium nickel-manganese-cobalt oxide (LiNMC) and lithium iron phosphate (LiFePO$_4$) batteries to offer an optimal trade-off between the energy loss and the charging time. The effects of the battery maximum charging voltage, ambient charging temperature and battery health status are analyzed. Zhang et al. [21] use the dynamic programming (DP) method to solve the trade-off problem concerning the charging time and the energy loss. A database based optimization approach is also proposed to decrease the computation time during the optimization process. These two strategies have balanced the charging time and the charging efficiency, while the battery temperature during the charging process is not considered. It should be noted that the battery temperature is a key factor for battery charging as too high or low temperature would harm the battery.

Abdollahi et al. [22] propose a closed-form optimal control solution to solve the optimal charging of a Li-ion battery. An objective function which considers the time-to-charge, energy losses and a temperature rise index is used to acquire the optimal CCCV solution. But some model parameters such as internal resistance are assumed to be constant in calculating the optimal charging current, this however will inevitably affect the efficacy of the method as variations of the battery internal resistance cannot be ignored due to its significant impact on the battery performance [23]. In addition, this strategy only considers the objective function for the CC stage in order to apply the variational method, and this inevitably affects the efficiency of the CV stage due to the fact

that the current profile at the CC stage is derived separately using a different objective function. As a result, the CCCV charging is unlikely optimal as a whole. It is therefore vital to optimize the whole CCCV process to achieve a desirable performance.

In this paper, we propose to simultaneously consider the battery charging time, energy loss and battery temperature rise (both interior and surface) as three conflicting objectives, and a triple-objective function based on a battery coupled thermoelectric model is formulated. Our goal is to design a battery optimal charging strategy to determine an optimal CCCV profile with a satisfactory trade-off among the three conflicting objectives. This is however a challenging and difficult issue. Our earlier study [24] proposes the coupled thermoelectric battery model where the battery thermal behavior especially the battery internal temperature and electric behavior (SOC and voltage) are simultaneously considered. Besides, variable parameters such as the internal resistances can be calculated for different operation conditions. Based on our early developed thermoelectric model, this paper first proposes a multiple triple-objective function which is optimized under highly time varying and nonlinear conditions, subject to various battery constraints, such as the battery SOC, voltage, current and some other physical limits during the operation. Then, meta-heuristic methods, in particular a modified TLBO algorithm, are applied to solve the nonlinear, time varying complicated battery charging problem. The effects of different weight settings in the objective function, including charging time weight, energy loss weight and temperature rise weight on the battery charging results are also evaluated and analyzed.

The remainder of this paper is organized as follows. The coupled thermoelectric model for a LiFePO$_4$ battery and the corresponding battery parameters are proposed in Section 2. Section 3 presents the triple-objective function and the corresponding constraints for the battery charging process. Then the principles of TLBO and the detailed implementation procedure for battery optimal charging strategy (charge current optimization) are presented in Section 4. Section 5 gives the experiment results including the comparison of optimization methods and verification of the optimal strategy, where the impacts of various weights on the battery charging performance are also analyzed. Finally, Section 6 concludes the paper.

2. LiFePO$_4$ battery model and parameters

In this section, the battery coupled thermoelectric battery model is presented firstly, followed by the illustration of corresponding parameters for the proposed coupled model.

2.1 LiFePO₄ battery thermoelectric model

2.1.1 Battery RC electric sub-model

Various battery models have been proposed so far, including black-box models (e.g., stochastic fuzzy neural network model [16]), grey-box models (e.g., electrical circuit model [25]), and white-box models (e.g., battery electrochemical model [26]). The dynamics of the electrical states of Li-ion batteries can be precisely modeled using electrical battery models. These electrical models use resistances or a combination of a resistance and RC-elements connected in series with a voltage source [24,27]. A second-order RC electric circuit model, shown in Fig.1, is adopted to represent the electric dynamics of the LiFePO₄ battery in this study.
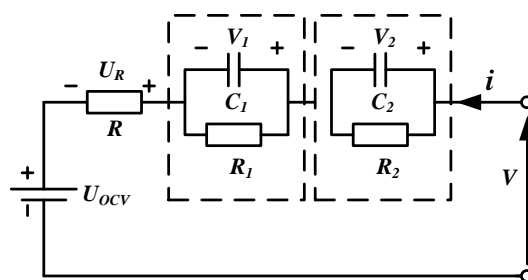
Fig.1. Battery RC electric circuit model.

The second-order RC model is comprised of a battery open circuit voltage U_{OCV}, a battery internal resistance R, and two battery resistance-capacitance ($R_1 C_1$, $R_2 C_2$) networks connected in series. U_{OCV} is the battery ideal voltage source representing the open-circuit behavior of a battery. The internal resistance R stands for the electrical resistance of different battery units with the loss and accumulation in the electrical double-layer, it mainly represents the resistive behavior of the electrolyte and contacts etc. The resistances R_1, R_2 and capacitances C_1, C_2 account for the battery diffusion resistances and diffusion capacitances respectively. It is generally believed that the first RC-element is related to the charge transfer processes occurring in the middle of the frequency range, while the second RC-element is responsible for reproducing the diffusion processes.

Suppose the injected current i remains constant during the same sampling time period, then the battery SOC level, the voltages of RC networks V_1, V_2, the battery terminal voltage V can be calculated using

$$\begin{cases} soc(k) = soc(k-1) - T_s/C_n * i(k-1) \\ V_1(k) = a_1 * V_1(k-1) - b_1 * i(k-1) \\ V_2(k) = a_2 * V_2(k-1) - b_2 * i(k-1) \\ V(k) = V_1(k) + V_2(k) + i(k) * R + U_{OCV} \end{cases} \tag{1}$$

where $a_j = \exp(-T_S/(R_j * C_j))$, $b_j = R_j * (1 - a_j)$, $j = 1,2$. C_n is the battery nominal capacity (unit: Ampere hour [Ah]), T_s is the sampling time period (unit: second [s]), and the value of U_{OCV} is a function of the battery SOC level.

2.1.2 Battery lumped thermal sub-model

It is assumed that the battery thermal sub-model mainly consists of two parts, namely the thermal transfer and thermal generation. The thermal conduction is supposed to be the only thermal transfer type within and outside the battery. The heat generation is uniformly distributed within the battery. The battery internal temperature and surface temperature are both supposed to be uniform, then a two-stage approximation of the radially distributed thermal model for the battery cells can be described as

$$\begin{cases} D_1 * \dot{T}_{in} = i^2 * R + k_1 * (T_{sh} - T_{in}) \\ D_2 * \dot{T}_{sh} = k_1 * (T_{in} - T_{sh}) + k_2 * (T_{amb} - T_{sh}) \end{cases} \tag{2}$$

where D_1 and D_2 are the battery internal and surface thermal capacity respectively. T_{in} and T_{sh} represent the battery internal and surface temperature respectively. $\dot{T}_{in}$ and $\dot{T}_{sh}$ represent $\dot{T}_{in} = dT_{in}/dt$, $\dot{T}_{sh} = dT_{sh}/dt$ respectively. T_{amb} denotes the battery ambient temperature. k_1 and k_2 are the battery thermal conduction coefficients.

Here, we adopt a simplified equation $Q = i^2 * R$ to calculate the battery generated thermal power, where Q is the battery thermal dissipation. Let $\dot{T}(k + 1) = (\frac{z-1}{T_s}) * T(k) = \frac{1}{T_s} * (T(k + 1) - T(k))$, the two-stage thermal sub-model for the LiFePO$_4$ battery can be finally described as

$$\begin{cases} T_{in}(k + 1) = (1 - T_s * k_1/D_1) * T_{in}(k) + T_s * k_1/D_1 * T_{sh}(k) + T_s/D_1 * i^2(k) * R \\ T_{sh}(k + 1) = T_s * k_1/D_2 * T_{in}(k) + (1 - T_s * (k_1 + k_2)/D_2) * T_{sh}(k) + k_2 * T_s * T_{amb}/D_2 \end{cases} \tag{3}$$

2.1.3 Battery coupled thermoelectric model

Following the introduction of the battery RC electric sub-model and lumped thermal sub-model, a battery coupled thermoelectric model can be achieved by combining Eq.(1) and Eq.(3) shown as follows,

$$\begin{cases} x(k + 1) = A * x(k) + B(k) \\ V(k) = V_1(k) + V_2(k) + R * i(k) + U_{ocv} \end{cases} \tag{4}$$

where

$$x(k) = [soc(k), V_1(k), V_2(k), T_{in}(k), T_{sh}(k)]^T$$

$$A = \begin{bmatrix} 1 & 0 & 0 & 0 & 0 \\ 0 & a_1 & 0 & 0 & 0 \\ 0 & 0 & a_2 & 0 & 0 \\ 0 & 0 & 0 & 1 - T_s * k_1/D_1 & T_s * k_1/D_1 \\ 0 & 0 & 0 & T_s * k_1/D_2 & 1 - T_s * (k_1 + k_2)/D_2 \end{bmatrix}$$

$$B(k) = [-T_s/C_n * i(k), \quad -b_1 * i(k), \quad -b_2 * i(k), \quad R * T_s * i^2(k)/D_1, \quad k_2 * T_s * T_{amb}/D_2]^T$$

This coupled thermoelectric model can simultaneously represent the interactions between the battery electric and thermal behaviors. With this model, the battery specific triple-objective function considering both the battery electrical and thermal behaviors especially the battery internal temperature can be formulated. Some parameters in this coupled model such as resistances can also be identified under different operation conditions (e.g. battery surface and internal temperatures, SOC level) to improve the optimization performance.

2.2 LiFePO$_4$ battery testing parameters

In order to design the battery optimal charging strategy, the first key step is to identify the parameters of the battery coupled thermoelectric model. Under laboratory test conditions, a LiFePO$_4$ battery cell which has a nominal operation voltage 3.2V and a nominal capacity 10Ah is used in this study. According to our experimental characterization and model identification at different SOC and temperature levels, we find that k_1, C_1, k_2, C_2, $\tau_2 = R_2 * C_2$ in Eq.(4) can be assumed constant. Other variable parameters have following features: 1) Resistance R depends primarily on the temperature and only varies slightly with SOC (normally EV batteries are only cycled in a limited range, where R does not change much as the SOC varies). The internal temperature directly affects the battery performance. Therefore we consider R is a function of the internal temperature; 2) Resistances R_1, R_2, however, depend on both the internal temperature and SOC, especially at low SOC level, R_1 and R_2 increase noticeably; 3) The battery time constant of the $R_1 C_1$ network, $\tau_1 = R_1 * C_1$, depends on the battery SOC level; 4) Battery open circuit voltage U_{OCV} depends on the battery SOC level.

The same method used to identify the model parameters in our previous work [24] is applied here. The battery internal resistance R is identified by a least square (LS) method under various internal temperature T_{in} and the relationship between $R = f_R(T_{in})$ and different internal temperatures is shown in Table 1. The battery resistances R_1 and R_2 are calculated under different internal temperatures and different battery SOC levels. The relationship between battery resistances R_1, R_2 and different situations are shown in Tables 2 and 3 respectively. Table 4 illustrates the relationship between the time constant $\tau_1 = R_1 * C_1$ and different battery SOC levels.

Table 1.

Battery resistance R[ohm] under different battery internal temperature T_{in}

T_{in} [°C]	-10	0	10	23	32	39	52
R[mΩ]	0.0259	0.0180	0.0164	0.0152	0.0125	0.0124	0.0120

Table 2.

Battery resistance R_1[ohm] under different battery internal temperature T_{in} and SOC levels

SOC	0 °C[ohm]	10 °C[ohm]	23 °C[ohm]	32 °C[ohm]	39 °C[ohm]	52 °C[ohm]
0.9	0.0067	0.0047	0.0037	0.0030	0.0032	0.0035
0.79	0.0093	0.0067	0.0046	0.0036	0.0033	0.0026
0.69	0.0098	0.0078	0.0048	0.0040	0.0037	0.0031
0.587	0.0134	0.0087	0.0057	0.0046	0.0041	0.0033
0.485	0.0195	0.0123	0.0080	0.0048	0.0043	0.0034
0.38	0.0271	0.0181	0.0123	0.0063	0.0057	0.0046
0.28	0.0369	0.0242	0.0155	0.0090	0.0082	0.0068
0.19	0.0369	0.0286	0.0196	0.0120	0.0111	0.0093
0.09	0.0370	0.0287	0.0234	0.0162	0.0148	0.0123
0.05	0.0371	0.0287	0.0300	0.0167	0.0161	0.0150

Table 3.

Battery resistance R_2[ohm]under different battery internal temperature T_{in} and SOC levels

SOC	0 °C[ohm]	10 °C[ohm]	23 °C[ohm]	32 °C[ohm]	39 °C[ohm]	52 °C[ohm]
0.9	0.0098	0.0057	0.0034	0.0043	0.0034	0.0016
0.79	0.0070	0.0062	0.0030	0.0040	0.0040	0.0024
0.69	0.0068	0.0044	0.0029	0.0043	0.0037	0.0020
0.587	0.0083	0.0047	0.0029	0.0040	0.0032	0.0017
0.485	0.0116	0.0070	0.0041	0.0035	0.0029	0.0018
0.38	0.0117	0.0079	0.0053	0.0042	0.0041	0.0038
0.28	0.0099	0.0065	0.0055	0.0065	0.0056	0.0040
0.19	0.0412	0.0180	0.0058	0.0076	0.0066	0.0048
0.09	0.0413	0.0181	0.0231	0.0077	0.0073	0.0066
0.05	0.0415	0.0181	0.0232	0.0087	0.0121	0.0230

Table 4.

Battery τ_1 under different SOC levels

SOC	0.1	0.2	0.3	0.4	0.5	0.6	0.7	0.8	0.9
τ_1	50	35	30	30	25	25	20	15	10

As for the battery OCV, the battery voltages after one-hour relaxation during the charging and discharging process under a certain SOC level are taken as the battery charging and discharging OCV respectively. Their average value is finally used as the battery OCV shown in Table 5.

Table 5.
Battery OCV[V] under different SOC levels

SOC	U_{OCV} [V](charge)	U_{OCV} [V](discharge)	U_{OCV} [V](average)
0.9	3.3303	3.3503	3.3403
0.79	3.3232	3.3401	3.3317
0.69	3.2989	3.3171	3.308
0.587	3.2922	3.3071	3.2996
0.485	3.2896	3.3048	3.2972
0.38	3.2759	3.2996	3.28775
0.28	3.2481	3.2775	3.2628
0.19	3.2170	3.2422	3.2296
0.09	3.0647	3.2154	3.14005
0.05	3.0234	3.2154	3.1194

After identification at different situations, the unknown parameters $R = f_R(T_{in})$, $R_1 = f_R(T_{in}, SOC)$, $R_2 = f_R(T_{in}, SOC)$, $\tau_1 = f_{\tau_1}(SOC)$ and $U_{OCV} = f_{ocv}(SOC)$ in the model can be calculated by the linear interpolation method based on the data listed in Tables 1 to 5 respectively. The constant parameters for the battery coupled thermoelectric model can be identified by the LS method based on the measured battery data. Details about the data used for the identification and the corresponding identification process can be found in our previous work [24] and will not be given due to the space limitation. The identification results of the constant parameters are shown in Table 6.

Table 6.
Parameter identification results for electric-thermal model

Parameter	Value
τ_2	598
D_1	286.35
D_2	30.9
k_1	1.6423
k_2	0.3102

3 Triple-objective optimal charging formulation

In this section, we present a triple-objective function based on our battery coupled thermoelectric model. This triple-objective function consists of three terms, including the battery charging time, energy loss and both the

battery internal and surface temperature rises. Besides, some constraints are also considered during the battery charging process.

3.1 Triple-objective function

To formulate the battery charging as an optimization problem, some performance indicators need to be defined. The battery charging time is a key charging performance indicator and it is preferred to be as short as possible. Another key indicator is the battery energy loss (power consumption) during the charging process. Large energy loss results in low battery charging efficiency. The battery charging time and energy loss are however two conflicting objectives. In addition, the rise of both battery interior and surface temperatures during the charging process is also an important indicator that has to be considered in the charging process. It should be noted that the difference of the battery internal and surface temperatures can be quite significant during the charging process. Excessive temperature especially the internal temperature leads to remarkable damage to the battery performance and service life, and can even lead to severe safety problem [24]. Therefore, the battery charging time, energy loss and temperature rise (both the interior and surface) should be taken into account in the objective function for optimizing the charging process.

With the battery coupled thermoelectric model introduced in Section 2.1, the cost functions relating to the battery charging time (CT) and energy loss (EL) can be calculated respectively as follows:

$$J_{CT} = T_s * k_{tf} \tag{5}$$

$$J_{EL} = T_s * \sum_{k=0}^{k_{tf}} (i^2(k) * R(k) + \frac{V_1^2(k)}{R_1(k)} + \frac{V_2^2(k)}{R_2(k)}) \tag{6}$$

where J_{CT} and J_{EL} are the cost function for CT and EL respectively. T_s is the sampling time period (in seconds) during the battery charging process and k_{tf} denotes the time when the battery capacity reaches its final target. $T_s * k_{tf}$ therefore accounts for the battery charging time. The voltages of the two RC networks, V_1, V_2 can be calculated based on Eq.(4) respectively.

Considering the battery lumped thermal model Eq.(3), we can simply define the battery internal temperature rise index $\tilde{T}_{in}(k) = T_{in}(k) - T_{amb}$ and the battery surface temperature rise index $\tilde{T}_{sh}(k) = T_{sh}(k) - T_{amb}$ accordingly. Substituting $\tilde{T}_{in}(k)$ and $\tilde{T}_{sh}(k)$ into Eq.(3), the relationship for these two temperature rise indexes can be formulated as

$$\begin{cases} \tilde{T}_{in}(k+1) = (1 - T_s * k_1/D_1) * \tilde{T}_{in}(k) + (T_s * k_1/D_1) * \tilde{T}_{sh}(k) + T_s * R(k) * i^2(k)/D_1 \\ \qquad = A_1 * \tilde{T}_{in}(k) + B_1 * \tilde{T}_{sh}(k) + C * R(k) * i^2(k) \\ \tilde{T}_{sh}(k+1) = (T_s * k_1/D_2) * \tilde{T}_{in}(k) + (1 - T_s * (k_1 + k_2)/D_2) * \tilde{T}_{sh}(k) \\ \qquad = A_2 * \tilde{T}_{in}(k) + B_2 * \tilde{T}_{sh}(k) \end{cases} \quad (7)$$

Assuming $T_{in}(0) = T_{amb}$ and $T_{sh}(0) = T_{amb}$, we have $\tilde{T}_{in}(0)=0$, $\tilde{T}_{sh}(0)=0$.

The cost function J_{TR} for the battery internal temperature rise (J_{TinR}) and surface temperature rise (J_{TshR}) can be defined as

$$J_{TR} = J_{TinR} + J_{TshR} = T_s * (\sum_{k=0}^{k_{tf}} \tilde{T}_{in}(k) + \sum_{k=0}^{k_{tf}} \tilde{T}_{sh}(k)) \quad (8)$$

The final objective function J_{charge} is a combination of these three cost functions J_{CT}, J_{EL} and J_{TR}. In other words,

$$J_{charge} = J_{CT} + J_{EL} + J_{TR}$$
$$= T_s * k_{tf} + T_s * \sum_{k=0}^{k_{tf}} \left(i^2(k) * R(k) + \frac{V_1^2(k)}{R_1(k)} + \frac{V_2^2(k)}{R_2(k)} \right) + T_s * (\sum_{k=0}^{k_{tf}} \tilde{T}_{in}(k) + \sum_{k=0}^{k_{tf}} \tilde{T}_{sh}(k)) \quad (9)$$

where the sampling time period T_s for this battery charging process is 1 second. The variable parameters can be achieved by the linear interpolation [24,28] and all terms in this triple-objective function J_{charge} can be calculated based on the previously introduced battery coupled thermoelectric model.

3.2 Constraints and CCCV optimization formulation

The optimization goal of the battery charging process is to find the suitable charging current profile $i(k)$ to minimize this triple-objective function J_{charge} during the battery charging process. Hard constraints such as voltage, current and battery SOC level limits need to be met during the optimal charging process. The target of the battery optimal charging strategy can be described as follows.

Minimize the triple-objective function J_{charge}, subject to:

$$\begin{cases} soc(k) = soc(k-1) - T_s/C_n * i(k-1) \\ V_1(k) = a_1 * V_1(k-1) - b_1 * i(k-1) \\ V_2(k) = a_2 * V_2(k-1) - b_2 * i(k-1) \\ \tilde{T}_{in}(k+1) = A_1 * \tilde{T}_{in}(k) + B_1 * \tilde{T}_{sh}(k) + C * R(k) * i^2(k) \\ \tilde{T}_{sh}(k+1) = A_2 * \tilde{T}_{in}(k) + B_2 * \tilde{T}_{sh}(k) \end{cases} \quad (10)$$

$$V(k) = V_1(k) + V_2(k) + i(k) * R(k) + U_{OCV} \quad (11)$$

$$\begin{cases} soc(0) = s_0 \qquad soc(t_f) = s_{t_f} \\ \tilde{T}_{in}(0) = 0 \qquad \tilde{T}_{sh}(0) = 0 \end{cases} \quad (12)$$

$$\begin{cases} i_{min} \leq i(k) \leq i_{max} \\ V_{min} \leq V(k) \leq V_{max} \end{cases} \tag{13}$$

where the s_0 and s_{t_f} are the initial SOC state and final SOC state during battery charging process respectively. The i_{min} and i_{max} stand for the lower and upper bound limits of charge current $i(k)$, and $V(k)$ is the battery terminal voltage. The V_{min} and V_{max} stand for the minimum and maximum bounds of $V(k)$. In addition, the s_0 and s_{t_f} should be defined between 0 and 1 to represent the corresponding SOC level, whereas during the whole charging process, the voltage should not exceed the upper terminal voltage bound V_{max}. Generally speaking, V_{max} is usually larger than the battery U_{OCV} at the SOC target, and it is less than the upper limit of the battery voltage to avoid overcharging.

In order to solve this optimal charging problem, we divide the battery charging process into two stages: a CC charging stage and a CV charging stage. During the CC stage, the terminal battery voltage begins to increase until it reaches the upper terminal voltage bound V_{max}. After this, the battery begins to be charged at the CV stage until the battery capacity meets the required SOC target. It is also assumed that the battery terminal voltage $V(k)$ rises up to the maximum bound V_{max} at time k_{cc} and then the charging process is switched into the CV stage. During the CV stage, the battery is charged at a constant voltage. The battery voltage is often maintained by power electronics in the charger while the current gradually decreases, and the dynamics of the CV stage charging current $i_{CV}(k)$ is formulated as follows,

$$i_{CV}(k) = (V_{max} - V_1(k) - V_2(k) - U_{OCV})/R(k) \tag{14}$$

At the CV stage, until the battery reaches the final charging state s_{t_f} for $k = k_{cc}, k_{cc} + 1, \dots k_{tf}$, the battery terminal voltage is fixed at the constant value V_{max} and other elements including $V_1(k), V_2(k), U_{OCV}, R(k)$ are also calculated using the coupled thermoelectric model. The charge current profiles $i_{CV}(k)$ in this stage are calculated by Eq.(14). Then the objective function J_{charge_CV} in the CV stage is calculated based on the charge current profiles $i_{CV}(k)$.

As stated above, the goal of the battery optimal charging strategy can be defined as a new equivalent optimization problem described as follows,

Minimize $J_{charge} = J_{charge\_CC} + J_{charge\_CV}$

$$J_{charge\_CC} = w_t * T_s * k_{cc} + w_E * T_s * \sum_{k=0}^{k_{cc}-1} f_{EL}(k) + w_T * T_s * \sum_{k=0}^{k_{cc}-1} f_{TR}(k) \tag{15}$$

$$J_{charge\_CV} = w_t * T_s * (k_{tf} - k_{cc}) + w_E * T_s * \sum_{k=k_{cc}}^{k_{tf}} f_{EL}(k) + w_T * T_s * \sum_{k=k_{cc}}^{k_{tf}} f_{TR}(k) \qquad (16)$$

Subject to:

$$\begin{cases} soc(0) = s_0 & soc(t_f) = s_{t_f} \\ \tilde{T}_{in}(0) = 0 & \tilde{T}_{sh}(0) = 0 \end{cases} \qquad (17)$$

$$\begin{cases} i_{min} \leq i(k) \leq i_{max} \\ V_{min} \leq V(k) \leq V_{max} \end{cases} \qquad (18)$$

where $f_{EL}(k) = i^2(k) * R(k) + V_1^2(k)/R_1(k) + V_2^2(k)/R_2(k)$, $f_{TR}(k) = w_{in} * \tilde{T}_{in}(k) + w_{sh} * \tilde{T}_{sh}(k)$; k_{cc} is the time for battery terminal voltage $V(k)$ first reaches the constant voltage V_{max}. k_{tf} is the time for the battery reaches its final charge state. w_t is the battery charging time weight, w_E is the battery energy loss weight, w_T is the battery temperature rise weight, w_{in} and w_{sh} stand for the two battery temperature weights (one for interior temperature and the other for the surface temperature) respectively.

This optimization problem aims to find a proper charge current profile $i_{CC}(k)$ at the CC stage which can minimize the J_{charge} for total battery charging process. It should be noticed that once $i_{CC}(k)$ is determined by an optimization algorithm, the values of k_{cc} and k_{tf} are determined accordingly. Then parameters including the resistances $R(k), R_1(k), R_2(k)$, voltage $V_1(k), V_2(k)$ and temperature rises $\tilde{T}_{in}(k)$, $\tilde{T}_{sh}(k)$ which are used in calculating the objective functions J_{charge_CC} and J_{charge_CV} can also be obtained using the battery coupled thermoelectric model. In other words, the charging current at the CC stage determines the battery charging time, energy loss and temperature rise (both the battery interior and surface) and further determines the value of the battery triple-objective function J_{charge}. The charging current profile $i_{CC}(k)$ thus plays an important role in the whole battery charging process and is chosen as our decision variables in minimizing the triple-objective function J_{charge}.

In summary, the fitness functions J_{charge_CC} in CC stage and J_{charge_CV} in CV stage are both considered for the battery optimal charging problem.

4. Optimal charging strategy

In order to solve the battery optimal charging problem formulated in Section 3, the heuristic method, namely the TLBO, and its variants are introduced in this section, then the detailed procedure for implementing the heuristic methods to find the battery optimal charging profile is presented.

4.1 Teaching-learning based optimization and its variants

Some parameters in the battery coupled thermoelectric model vary along the charging process, e.g. the battery OCV varies with the SOC level, and battery resistances R, R_1, R_2 also vary with the battery temperature and SOC level. The triple-objective function for the battery charging process has to be optimized under time varying and nonlinear conditions. This presents a significant challenge for traditional analytical optimization techniques such as the variational method to solve the complicated optimization problem. It calls for new tools to optimize these variables effectively. Meta-heuristic methods are generally flexible in solving non-convex non-linear problems and naturally immune to the irregular problem formulations and constraints. Among many heuristic methods developed so far, teaching-learning-based optimization (TLBO) is a latest powerful method free of specific parameter tunings proposed by Rao et al. [29] and has been applied in solving a number of single or multiple objectives industrial optimization problems [30,31]. The original TLBO and some efficient variants such as modified Teaching-learning based optimization (MTLBO) [32] and self-learning Teaching-learning based optimization (SL-TLBO) [33] are employed in this paper to solve the nonlinear, time-varying, complicated battery optimal charging problem.

TLBO is a population-based method which mimics the nature of the teaching and learning processes in a class. The optimization process includes two phases namely the teaching phase and the learning phase. In the teaching phase, a teacher is elected first in each learning generation and the students learn knowledge from this teacher. A learning phase is designed for students to learn from mutual interactions with counterparts to gain potential useful information. It is convenient and simple to adopt this optimization algorithm for battery optimal charging strategy since there are no algorithm specific parameters that need to be adjusted by user for the algorithm implementation. The general framework of TLBO for the value optimization is shown in Fig. 2 [34].

In this paper, instead of using analytic optimization methods, TLBO is adopted to search for the best charge current $i(k)$ in the constant-current (CC) process through its two phases, aiming to minimize the triple-objective function J_{charge} described in Section 3 and to obtain the suitable charge current profile for battery optimal charging.

Besides, some latest variants of TLBO including MTLBO and SL-TLBO, both of which are specialized in solution space exploitations, are also employed to make a comparison. The best performed algorithm will then be adopted to solve the battery charging optimization problem accordingly.
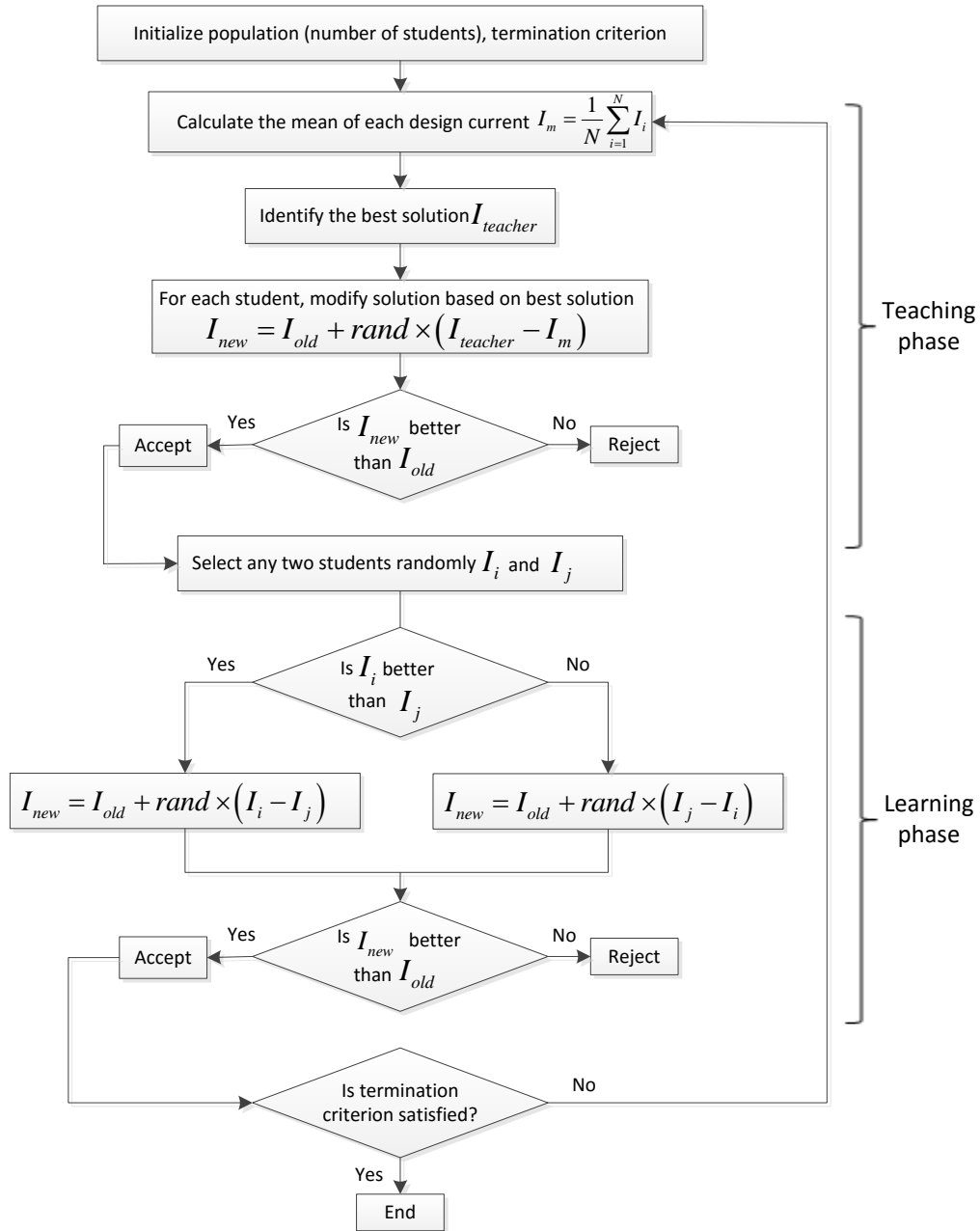
Fig. 2. General framework of TLBO for the value optimization

4.2 Implementation of heuristic methods for battery optimal charging problem

Fig. 3 illustrates the flowchart of implementation of the heuristic methods for the battery charging optimization problem. The main procedures are presented in details as follow.
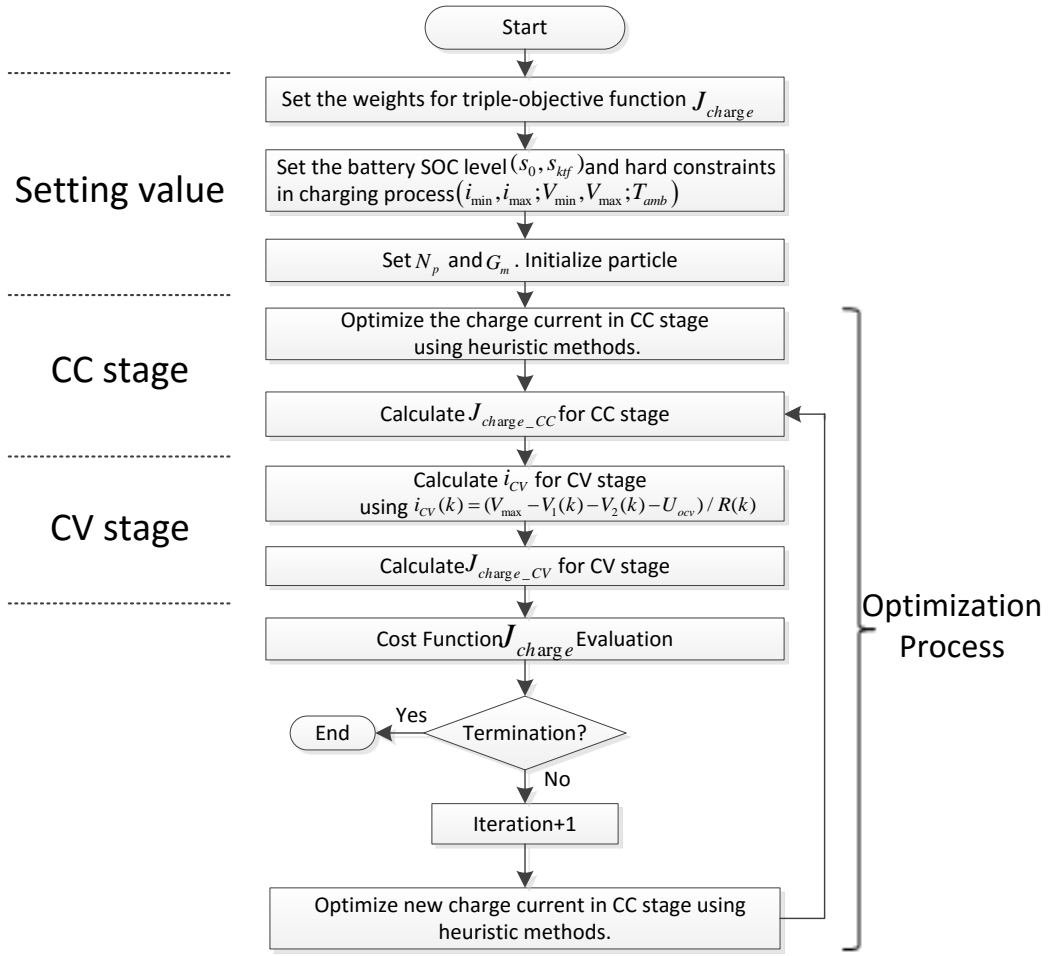
```
                              ┌──────────┐
                              │  Start   │
                              └────┬─────┘
                                   ▼
              ┌──────────────────────────────────────────────────┐
   Setting    │ Set the weights for triple-objective function J_charge │
    value      └──────────────────────┬───────────────────────────┘
```

Set the weights for triple-objective function J_{charge}

Set the battery SOC level (s_0, s_{ktf}) and hard constraints in charging process $(i_{min}, i_{max}; V_{min}, V_{max}; T_{amb})$

Set N_p and G_m. Initialize particle

Setting value

Optimize the charge current in CC stage using heuristic methods.

Calculate J_{charge_CC} for CC stage

CC stage

Calculate i_{CV} for CV stage using $i_{CV}(k) = (V_{max} - V_1(k) - V_2(k) - U_{ocv})/R(k)$

Calculate J_{charge_CV} for CV stage

CV stage

Cost Function J_{charge} Evaluation

Termination? → Yes → End

No

Iteration+1

Optimize new charge current in CC stage using heuristic methods.

Optimization Process

Fig. 3. Flowchart of implementing the heuristic methods for battery optimal charging strategy

Step 1: Set the charging time weight w_t, energy loss weight w_E, temperature rise weight w_T, internal and shell temperature weights w_{in} and w_{sh} in the battery triple-objective function J_{charge}.

Step 2: Set the battery charging initial SOC level s_0 and target SOC level $s_{k_{tf}}$ respectively. Set the hard constraints for battery charging process: i_{min} and i_{max} for charge current limits; V_{min} and V_{max} for terminal voltage limits; T_{amb} for battery ambient temperature.

Step 3: Set the population sizes N_p, numbers of generations G_m and the corresponding tuning parameters for the population-based heuristic methods (PSO, CFPSO,WPSO and SL-TLBO). Initialize the particles for heuristic methods.

Step 4: For $k = 1$ to k_{max} do

1) At the CC stage, calculate the objective fitness J_{charge_CC} in each generation using Eq.(15) until the terminal voltage reaches the maximum threshold V_{max}, then the battery charging process will enter to the CV stage.

2) At the CV stage, determine the charge current profile using Eq.(14) in each generation and then calculate the objective fitness J_{charge_CV} using Eq.(16) until the battery SOC level reaches its final state $s_{k_{tf}}$.

3) Evaluate the final triple-objective function J_{charge} according to the sub-objective fitness J_{charge_CC} and J_{charge_CV}. Check whether the maximum number of iterations is achieved, and the loop is terminated once the condition is met.

4) Update the charge current in CC stage using the corresponding heuristic methods. When the terminal voltage reaches V_{max}, terminate the CC stage; When the battery SOC level reaches $s_{k_{tf}}$ which means the battery has been charged to the targeted capacity, terminate the CV stage. When the termination criteria have been satisfied, terminate the whole optimization process.

where k_{max} is the maximum number of iterations.

According to the above procedure, the optimal CCCV charge current profile can be obtained. This resultant current profile can charge the battery SOC level from initial s_0 to final $s_{k_{tf}}$ with the minimal cost of triple-objective function J_{charge}. It balances the conflicts among the key indicators for the battery charging process. The numerical results achieved by the method are presented and analyzed in Section 5.

5 Results and discussion

In this study, comprehensive tests are first conducted based on the coupled battery thermoelectric model and the proposed battery optimal charging strategy presented in Section 4. The performance of the optimal charge current profile for the battery cell charging process is then analyzed. For the parameter settings, the sampling time period T_s is set to 1s. The maximum number of iterations k_{max} is 3000. In practice, the battery charging of the EVs/HEVs normally will start before the battery is fully discharged (SOC=0), as fully discharging will not only damage the life cycle of the battery, but also cause significant inconvenience to the users. On the other hand, in many applications, charging to 100% capacity is unnecessary due to the length of the charging time and travel necessity. Therefore, in this paper, the battery initial SOC level and the target level are selected as $s_0 =$

0.1 and $s_{k_{tf}}= 0.9$ respectively. The following hard constraints for battery charge current and terminal voltage are used: $i_{min} = -30A$, $i_{max} = 0A$, $V_{min} = 2.6V$, $V_{max} = 3.65V$. The ambient temperature during charging process is fixed as $T_{amb} = 29℃$. Three cases of tests are conducted, including (i) comparison study of various optimization methods; (ii) verification of the developed optimal charging strategy; (iii) study on the effects of various weights in the objective function.

5.1 Comparison study of various optimization methods

To choose an effective optimization algorithm, several population-based heuristic methods, including the basic TLBO, TLBO variants such as the SL-TLBO and MTLBO, as well as particle swarm optimization (PSO) and some PSO variants including WPSO, CFPSO [35] are compared in this case study. Moreover, the influence of the population sizes and the number of generations on the algorithm performance is investigated, including four population sizes 10, 20, 30 and 50, and the number of generations G_m varying from 20 to 60.

Table 7.

Comparisons of TLBO(SL-TLBO,MTLBO) and PSO(WPSO,CFPSO) for different G_m(number of generations) and N_p(number of population) in terms of J_{charge} (triple-objective function)

N_p	G_m	J_{charge}(TLBO)	J_{charge} (SL-TLBO)	J_{charge} (MTLBO)	J_{charge} (PSO)	J_{charge} (WPSO)	J_{charge} (CFPSO)
10	20	42623.328	42624.354	42622.158	42642.188	42637.737	42655.958
10	40	42623.328	42622.857	42622.009	42638.142	42631.306	42628.102
10	50	42622.536	42622.857	42622.009	42628.672	42624.626	42628.101
10	60	42622.280	42622.857	42622.009	42625.293	42623.388	42624.540
20	20	42626.515	42624.601	42622.011	42640.747	42629.518	42647.280
20	30	42622.088	42622.071	42622.009	42640.747	42629.518	42632.974
20	**50**	**42622.088**	**42622.028**	**42622.008**	42633.518	42624.699	42631.408
30	20	42622.850	42622.703	42622.132	42629.359	42631.993	42625.079
30	30	42622.286	42622.454	42622.010	42629.359	42627.397	42625.079
50	10	42623.252	42623.521	42622.236	42632.387	42629.895	42637.988
50	20	42622.742	42622.363	42622.020	42630.297	42627.508	42629.182

The comparative results of these algorithms for optimizing the battery charging objective function J_{charge} are listed in Table 7, where the average fitness values of 10 independent runs on J_{charge} by each optimization method are presented. The weights w_t, w_E, w_T, w_{in} and w_{sh} in objective function J_{charge} were all set to 1 in this experiment. The self-learning weighting factor of SL-TLBO was set to 3. The cognitive and social factors of both PSO and its variants were set to 2, and the constriction factor of CFPSO was set to 0.729. The weight w in

WPSO was chosen as the function defined as $w = 0.9 - 0.5 * (G/G_m)$, where G and G_m are the current generation index and the number of generations respectively.

It is clear from Table 7 that the basic TLBO and its variants SL-TLBO, MTLBO with different numbers of population produced better results of J_{charge} than the PSO and its variants WPSO, CFPSO. For the basic TLBO and its variants, different population sizes N_p and numbers of generations G_m would produce different optimal results for J_{charge}. The results of MTLBO under the same N_p, G_m are better than TLBO and SL-TLBO, which means that MTLBO is less sensitive to the parameter settings and is more robust. The strategy produced by the MTLBO with the population size $N_p = 20$ and the number of generations $G_m = 50$ gives the best result $J_{charge} = 42622.008$, it can even achieve adequate good results when the population size is small.
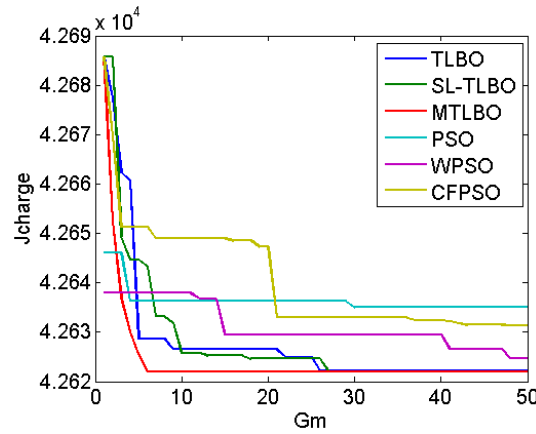

Fig. 4. Convergence characteristics of algorithms for battery triple-objective function optimization.

Fig. 4 illustrates the convergence rates of different algorithms. The curves are the battery triple-objective function J_{charge} values against the number of generations G_m. The population size N_p and generations number G_m are set to 20 and 50 respectively. The J_{charge} values in the graph are the averages of 10 independent runs. According to Fig. 4, the convergence speeds of the basic TLBO and its variants are faster than the PSO and its variants. Among the TLBO algorithms, MTLBO converges faster and produce better optimal results of the objective function. Accordingly, we choose MTLBO as the optimization algorithm for optimizing the battery charging objective function. N_p and G_m are set to 20 and 50 respectively in this paper in following experiments.

5.2 Verification of the proposed optimization strategy

We firstly divide the values of triple-objective function J_{charge} into battery charging time (J_{CT}), battery energy loss (J_{EL}) and battery temperature rise ($J_{TR} = J_{TinR} + J_{TshR}$) shown in Table 8. The values are calculated based on different selections of N_p and G_m to investigate the result of each sub-cost function when the weights w_t, w_E, w_T, w_{in} and w_{sh} in J_{charge} are all set to 1. It can be observed from Table 8 that in this test, values of J_{EL} and J_{TR} are much larger than J_{CT}, nearly up to sixteen-fold and twenty-fold respectively. To ensure that the sub-cost functions are fairly optimized, the following weights $w_t = 1$, $w_E = 0.1$, $w_T = 0.1$, $w_{in} = 0.5$, $w_{sh} = 0.5$ are used respectively, while the detailed impact of weight combinations will be addressed in sub-section 5.3.

Table 8.

Values of sub-cost function under different algorithm settings

N_p	G_m	J_{CT}	J_{EL}	J_{TR}	J_{TinR}	J_{TshR}
20	50	1170	16572.282	24879.726	13950.948	10928.778
10	60	1170	16572.464	24879.545	13950.776	10928.769
30	30	1170	16572.376	24879.634	13950.815	10928.819

After setting the appropriate weights for battery charging objective function J_{charge}, five different charging current profiles including the optimal current profile are compared to verify the performance of the charging current profile optimized by our strategy. These charging current profiles include the charging current trajectory during the CC stage until the battery terminal voltage reaches V_{max} and the charging current trajectory at the CV stage until the battery SOC reaches s_{t_f}. The optimal current profile is calculated based on our MTLBO algorithm, while other current profiles are calculated based on our coupled thermoelectric model with the charging current profile $i_{CC}(k)$ being chosen randomly. Fig. 5 illustrates the results of the battery terminal voltage and the battery temperature (both the interior and surface) on these five different current profiles during the charging process to bring battery SOC from 0.1 to 0.9. It can be observed that larger current in the CC stage shortens the battery charging time and the battery terminal voltage reaches the V_{max} (here is 3.65V) in a shorter time. However, both the battery internal temperature and surface temperature rise up to a higher level rapidly when larger charging currents are applied during the charging process.
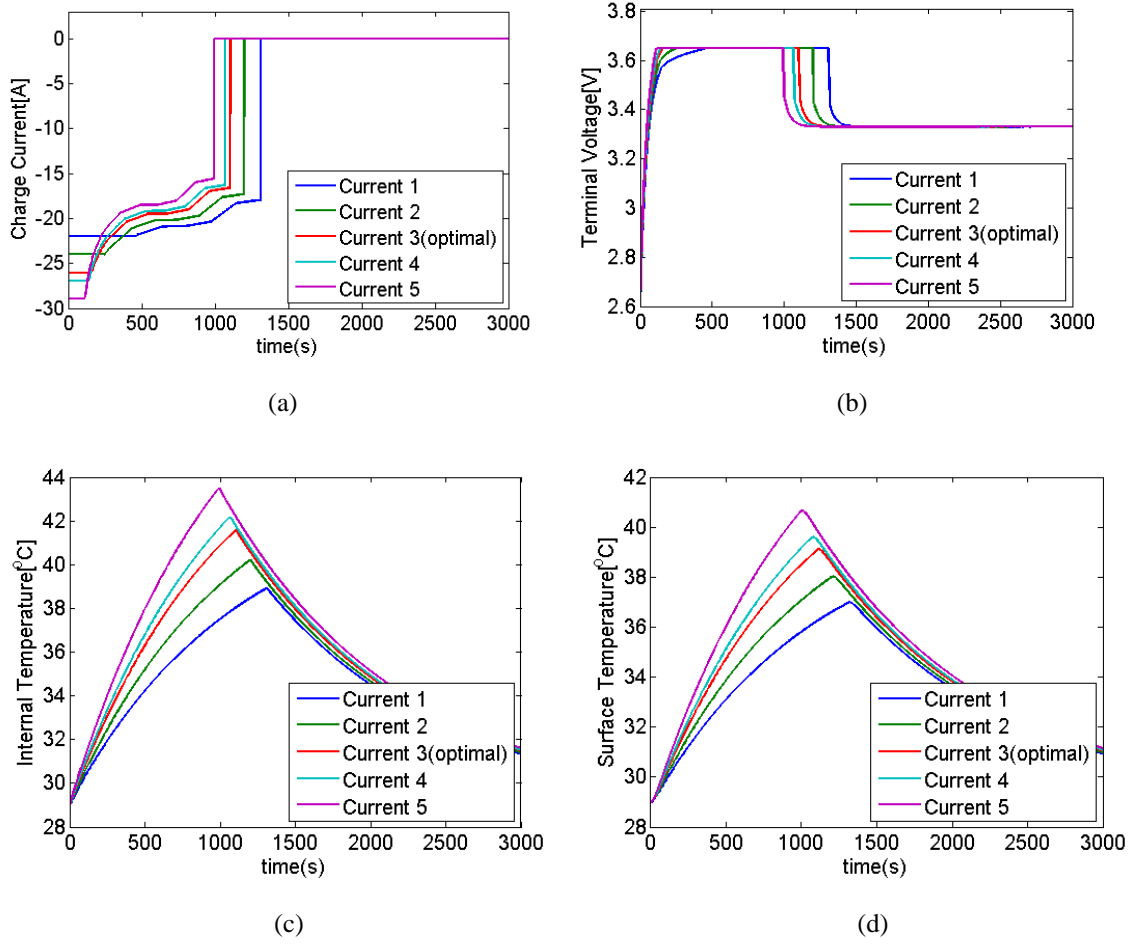
Fig. 5. Different battery charging profiles (including the optimal profile): a) charge current profiles b) terminal voltage profiles c) internal temperature profiles d) surface temperature profiles

The triple-objective function J_{charge} and its sub-cost functions including charging time, energy loss and temperature rise with corresponding weights for these five current profiles are shown in Fig. 6. It shows that the current profile 3 (optimal current) has the lowest value 4049.157 for J_{charge} compared with other current profiles. The triple-objective function J_{charge} based on these five current profiles are divided into three parts of sub-cost functions with corresponding weights and are listed in Table 9. It reveals that, apart from the optimal current profile, either reducing or adding the current in the battery charging CC stage lead to an increase of the triple-objective function J_{charge}. For current profiles 1-2, smaller currents in the CC stage reduce the value of J_{EL} during the battery charging process, but incur larger J_{CT} and J_{TR}, and further increase the cost function J_{charge} accordingly. For current profiles 4-5 with larger currents in the CC stage, J_{CT} is decreased during the battery charging process but J_{EL} and J_{TR} are increased significantly, further causing the rise of the overall cost function J_{charge} accordingly.
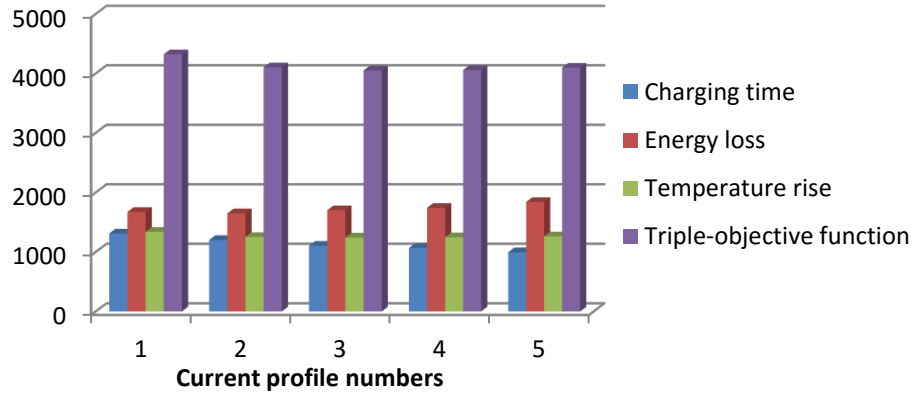
Fig. 6. Triple-objective function and its sub-cost functions with weight for different battery charge current profiles

Table 9.

Values of sub-cost function J_{CT}, J_{EL}, J_{TR} with weights and J_{charge} under some different charge current profiles

Current profile No.	$w_t * J_{CT}$	$w_E * J_{EL}$	$w_T * J_{TR}$	J_{charge}	I
1	1311	1672.701	1337.885	4321.586	-22
2	1201	1649.755	1252.199	4102.954	-24
3	1105	1701.569	1242.588	**4049.157**	**-26.088**
4	1068	1741.387	1247.621	4057.008	-27
5	995	1839.738	1261.570	4096.308	-29

5.3 Effects of triple-objective function weights

The weights in the battery triple-objective cost function J_{charge} are crucial for the design of the battery charging strategy. In this subsection, tests are conducted to investigate the effects of these weights on the performance of the charging process.

Tests with different weights for the charging time

The results of tests using different battery charging time weights value w_t ranging from 0.2 to 2.2 are shown in Fig.7. These results include the optimal charging current profiles and the corresponding variables (battery terminal voltage, internal temperature and shell temperature). The other weights in the triple-objective function are set constant with $w_E = 0.1$, $w_T = 0.1$, $w_{in} = 0.7$, $w_{sh} = 0.3$ (The battery internal temperature directly affects the battery performance so we empirically set w_{in} slightly larger than w_{sh}). It can be clearly seen that as w_t increases from 0.2 to 2.2, the total charging time which brings SOC from 0.1 to final state 0.9 becomes shorter due to the larger charge current profile. The optimal current in the CC stage is 29.969A when $w_t = 2.2$ compared with the value 24.636A when $w_t = 0.2$. In other words, a large w_t means more emphasis on the

battery charging time and less emphasis on the battery energy loss as well as battery temperature rise during the charging process, and vice versa. Besides, the battery terminal voltage goes up to the threshold V_{max} more quickly and the battery temperature (both the interior and surface) increases higher and faster as larger w_t is adopted.

It is also shown that when w_t exceeds 2.2, the optimal charge current in the CC stage is almost identical, and further increasing will not make noticeable difference to the battery charging current profiles. $w_t = 2.2$ is therefore taken as the upper limit case as the optimal charge current in the CC stage practically reaches its maximum threshold.
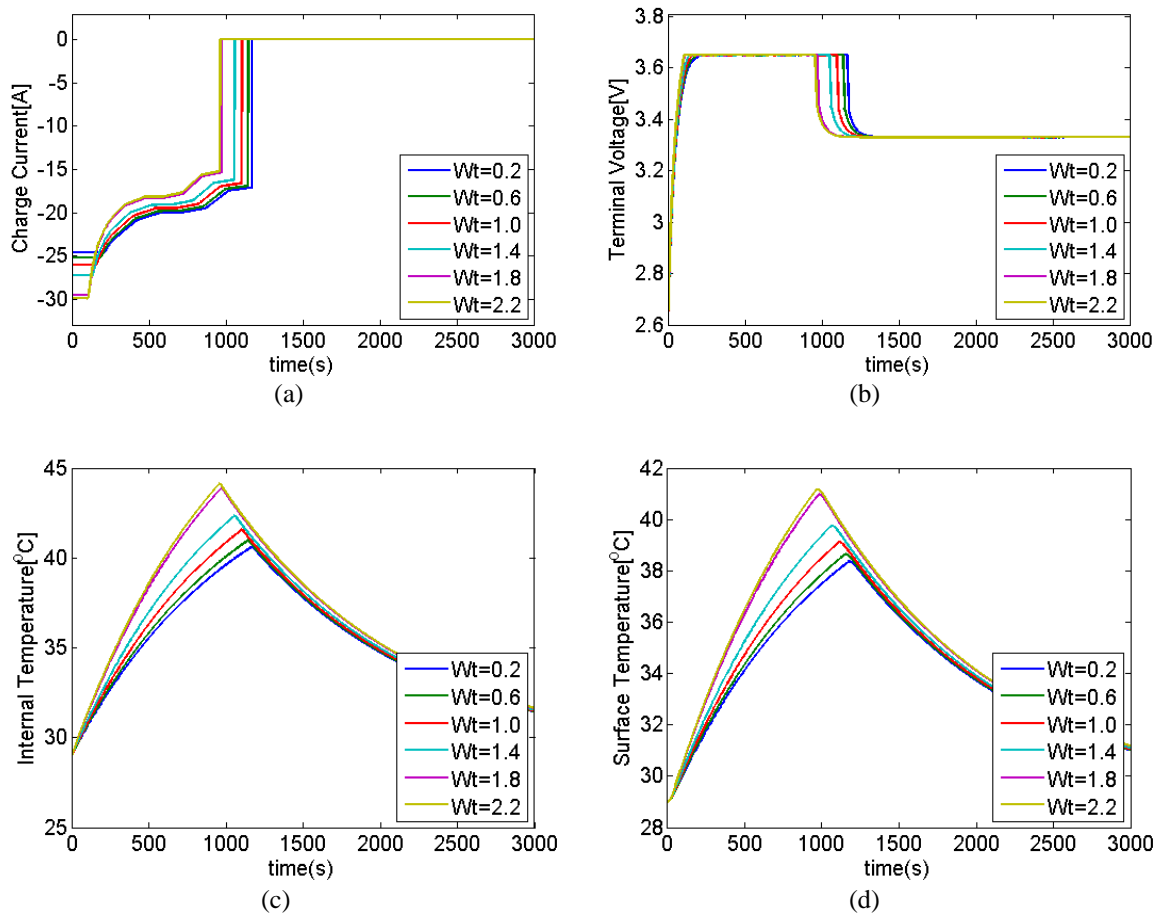

Fig. 7. Effect of different charging time weights w_t ($w_E = 0.1, w_T = 0.1, w_{in} = 0.7, w_{sh} = 0.3$)

Tests with different battery energy loss weights

Fig. 8 illustrates the effects of varying the weight for the battery energy loss in the triple-objective function on the battery charging performance. Here the weights for the battery charging time, battery temperature rise, battery internal and surface temperatures are fixed at $w_t = 0.1, w_T = 0.1, w_{in} = 0.7$ and $w_{sh} = 0.3$ respectively,

only the battery energy loss weight w_E varies. The primary role for weight w_E is to suitably emphasize the battery energy loss during the battery optimal charging process. As w_E is changed from 0.05 to 1.6, it can be observed that the optimal charge current in the CC stage gradually decreases from 29.440A ($w_E = 0.05$) to 23.921A ($w_E = 1.6$) to prolong the total battery charging time. Large w_E implies more emphasis on the battery energy loss and less emphasis on the battery charging time as well as battery temperature rise, which results in low charging current. It would further generate less energy loss to improve the charging efficiency, cause less rise on both battery interior temperature and surface temperature during the battery charging process. It is also shown that the battery charging current profiles will not change noticeably when w_E is outside the range of [0.05 1.6], therefore these boundary values are chosen as the lower and upper limits cases for w_E during this battery optimal charging process.
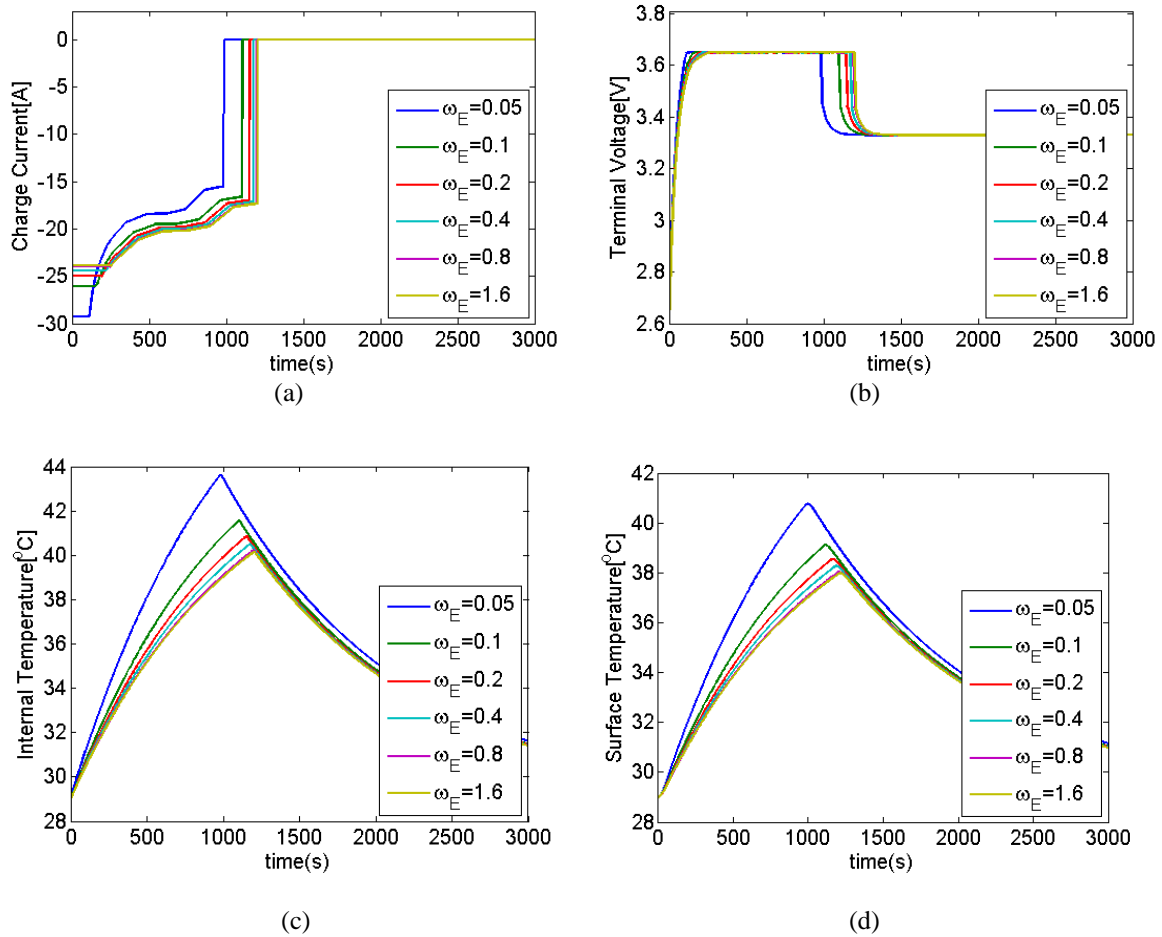

Fig. 8. Effect of different energy loss weights w_E ($w_t = 0.1$, $w_T = 0.1$, $w_{in} = 0.7$, $w_{sh} = 0.3$)

Tests with different battery temperature rise weight

Another test is conducted to investigate the effect of battery temperature rise weights w_T on the battery optimal charging performance, and the results are shown in Fig. 9. Here the battery charging time weight, battery energy loss weight and battery temperature weights were fixed to $w_t = 0.1$, $w_E = 0.1$, $w_{in} = 0.7$ and $w_{sh} = 0.3$ respectively. Six different battery temperature rise weights w_T (0.01, 0.05, 0.10, 0.50, 1.00, 5.00) were chosen in this test. When w_T increases from 0.01 to 5.00 gradually, the optimized charging current in the CC stage increases. Even though the battery internal temperature and surface temperature increase more rapidly under the increasing current with a larger w_T, the total charging time J_{CT} will be shortened and hence the sub-cost function J_{TR} will decrease accordingly. It can be observed from Fig. 9 that a lower value of w_T can cause slower battery temperature rise but longer charging time, hence leading to a larger J_{TR}, and vice versa. A high weight w_T means more emphasis on the battery temperature rise, which results in high level of charging currents in the CC stage, thus reducing the battery charging time and achieve low value for battery temperature rising J_{TR} through the whole battery charging process.
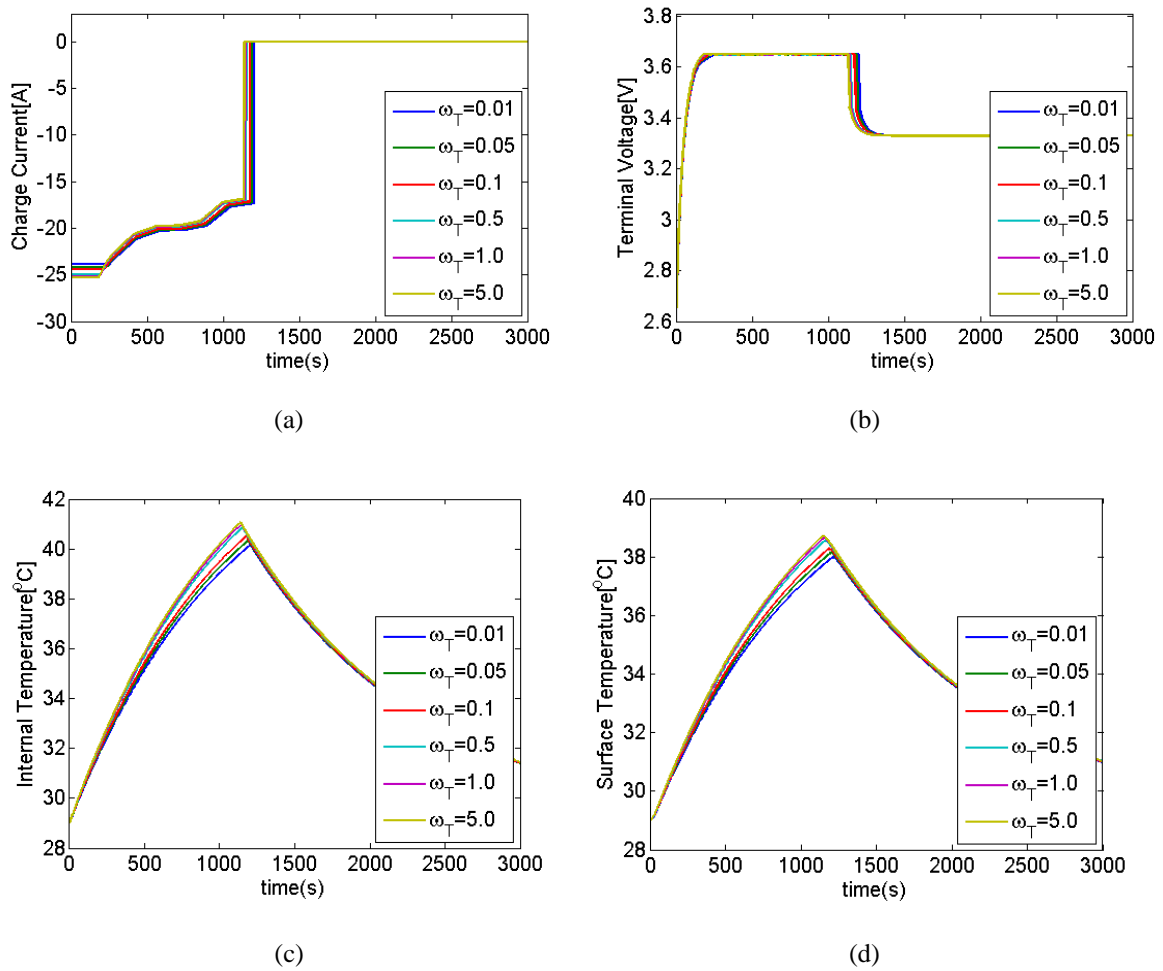

(a)

(b)

(c)

(d)

Fig. 9. Effect of different temperature rise weights w_T ($w_t = 0.1$, $w_E = 0.1$, $w_{in} = 0.7$, $w_{sh} = 0.3$)

The effects of varying temperature weight w_T on the value of each cost term in the triple-objective function are shown in Fig. 10. It is clear that there exists a range where the change of w_T has more significantly effects on the cost terms, and while outside the range, further increase of w_T has little impact on these cost terms. In detail, it is evident that for the charging time and temperature rise (both T_{in} rise and T_{sh} rise), the optimal value of the objective function decreases dramatically as w_T is increased from 0 to 1. However, as w_T is increased from 1 to 5, the optimal values do not change significantly. On the other hand, the energy loss is adversely affected by w_T, it increases sharply as w_T decreases, and then the increase of the energy loss slows down as w_T is increased beyond 1. Further increasing w_T above 5 will not make noticeable difference for the battery charging profiles and the cost terms are almost constant, which implies that 5 is the maximum threshold for w_T.
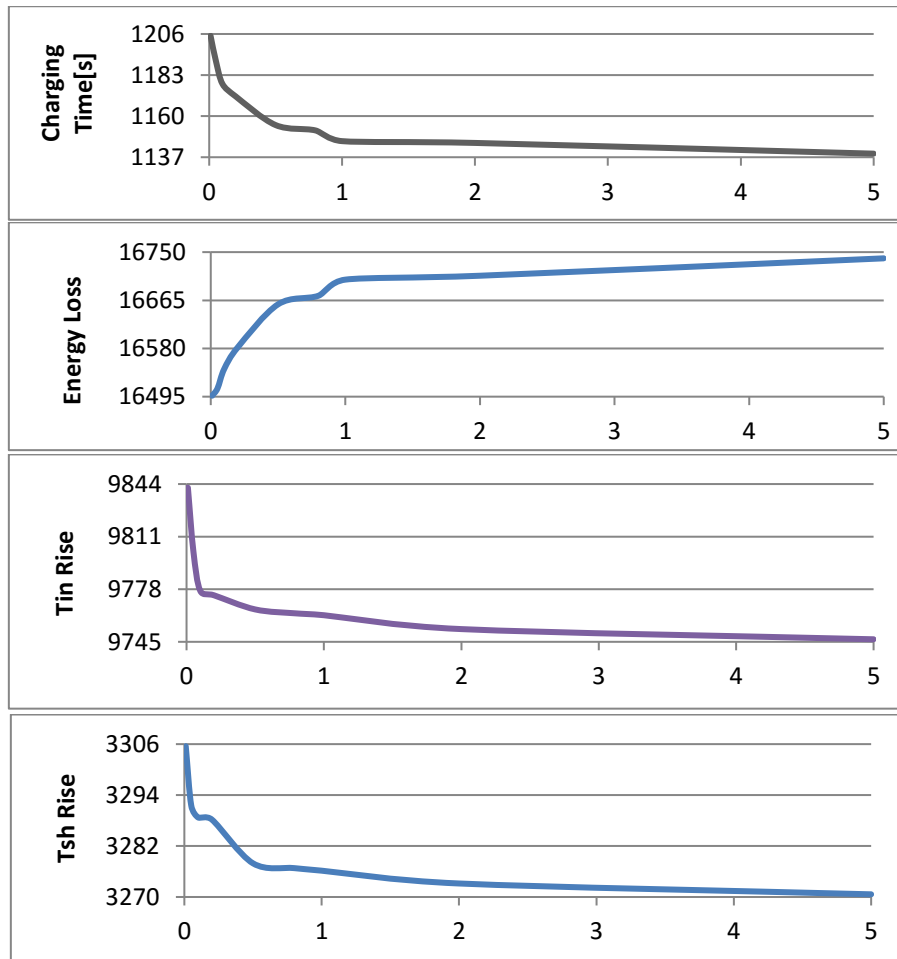

Fig. 10. Charging time J_{CT}, energy loss J_{EL}, temperature rise J_{TinR}, J_{TshR} for different values of w_T ($w_t = 0.1$, $w_E = 0.1$, $w_{in} = 0.7$, $w_{sh} = 0.3$)

As a result, different weights in the triple-objective function J_{charge} will lead to different battery optimal charging profiles. The battery charging time and energy loss are two conflicting goals. By adjusting the weights

for the sub-cost function terms, the charging current profiles with different emphasises on either the battery charging time, energy loss or temperature rise (both interior and surface) can be identified separately.

Generally speaking, in practice, EVs are mainly charged either at a charging station or at home. Charging EVs at a charging station is analogous to gasoline refueling for conventional vehicles. The customer requirement is often to charge the EVs within a short period that is comparable to the time needed for gasoline refueling of conventional vehicles. The priority is to use a relatively large charging current profile to achieve fast charging, thus a large w_t in the triple-objective function is required. On the other hand, for home charging, EV owners often charge EVs at night or during the off-peak periods, in favour of reduced costs and utilization of renewable energy, and the charging time is usually long (e.g., 6-8h) with low charging current. In this case, the priority in home charging could be the low energy loss which can be achieved by applying a large w_E in the triple-objective function. Besides, the battery temperature increases noticeably in high power high current applications. The difference between battery surface and internal temperature would be significant (e.g., sometimes greater than 10^oC). When the battery temperature exceeds the reliable operating range, battery performance will be severely damaged and even lead to battery failures and safety problems. So the temperature rise is one of the priorities in high power applications, and to low the temperature rise, the weight w_T in proposed charging strategy needs to be adjusted.

6. Conclusion

Charging strategy is a key issue in guaranteeing safe and effective operations of Li-ion batteries in electric vehicles. In this paper, an attempt has been made to apply heuristic methods especially the modified TLBO algorithm to optimize the LiFePO$_4$ battery charging profile. Due to the lack of considerations of the battery internal temperature in the existing published work, this paper has proposed a specific triple-objective function which has embedded three conflicting but important objectives: battery charging time, energy loss, and especially the battery interior temperature rise. Then a proper CCCV current profile as a result for the best trade-off of the triple objectives can be achieved by solving the highly nonlinear and time-varying optimization problem. It benefits from the universal optimization capability of the heuristic methods and the capture of the battery thermoelectric behavior using the coupled thermoelectric model. In the optimization procedure, different heuristic methods such as TLBO (both basic and variants), and PSO (both basic and variants) are compared. The results revealed that the MTLBO converges faster and produces better objective function values than other alternatives. The impacts of various weights for the charging time, energy loss, and temperature rise on the final

optimal charging current profiles are also investigated. By adjusting the weights of sub-cost terms in the triple-objective function, the charge current profiles with different priorities can be obtained by the proposed battery optimal charging strategy.

In summary, the main contributions of this work are as follows: 1) a triple-objective function is proposed, considering the battery charging time, energy loss, and particularly the internal temperature rise of batteries which is important for safe and efficient operation of electric vehicles, especially for some high power applications where the difference between surface and internal temperatures can be quite large. 2) Both the CC and CV stages can be holistically considered using the meta-heuristic methods to solve the time varying and nonlinear optimization problem, and the adopted thermoelectric model also helps to improve the accuracy by taking into consideration the couplings between the battery thermal and electrical behaviors. All these can help to achieve more reliable and realistic charging strategies for EVs. 3) Several heuristic methods for searching the optimal battery charging current profile by minimizing the triple-objective function are investigated and compared, and a modified TLBO has shown to outperform other counterparts. 4) Charging current profiles with different priorities can be achieved by adjusting the weights in the triple-objective function, which brings extra benefits in that the resultant current profile can meet different requirements for various battery applications. 5) The proposed charging strategy combines the novel but generic thermoelectric model and meta-heuristic optimization methods, which can be easily extended to other battery types. Therefore, the results presented in this paper are not only novel in the methodology development, but also significant in practical applications.

Acknowledgement

Reference

[1] L. Lu, X. Han, J. Li, J. Hua, M, Ouyang, A review on the key issues for lithium-ion battery management in electric vehicles. Journal of power sources 226 (2013) 272-288.

[2] B. G. Pollet, I. Staffell, J. Shang, Current status of hybrid, battery and fuel cell electric vehicles: From electrochemistry to market prospects, Electrochimica Acta 84 (2012) 235-249.

[3] M. Mastali, E. Samadani, S. Farhad, R. Fraser, M. Fowler, Three-dimensional Multi-Particle Electrochemical Model of LiFePO 4 Cells based on a Resistor Network Methodology. Electrochimica Acta 190 (2016) 574-587.

[4] C. Zhang, J. Jiang, Y. Gao, W. Zhang, Q. Liu, X. Hu, Polarization Based Charging Time and Temperature Rise Optimization for Lithium-ion Batteries. Energy Procedia 88 (2016) 675-681.

[5] M. Yilmaz, P. T. Krein, Review of battery charger topologies, charging power levels, and infrastructure for plug-in electric and hybrid vehicles. Power Electronics, IEEE Transactions on, 28(5) (2013) 2151-2169.

[6] Z. Rao, S. Wang, A review of power battery thermal energy management. Renewable and Sustainable Energy Reviews, 15(9) (2011) 4554-4571.

[7] B. Park, C. H. Lee, C. Xia, C. Jung, Characterization of gel polymer electrolyte for suppressing deterioration of cathode electrodes of Li ion batteries on high-rate cycling at elevated temperature, Electrochimica Acta 188 (2016) 78-84.

[8] C. Zhang, J. Jiang, Y. Gao, W. Zhang, Q. Liu, X. Hu, Charging optimization in lithium-ion batteries based on temperature rise and charge time. Applied Energy (2016).

[9] Battery Chargers and Charging Methods, 2016. URL, http://www.mpoweruk.com/chargers.htm

[10] J. Jiang, Q. Liu, C. Zhang, W. Zhang, Evaluation of acceptable charging current of power Li-ion batteries based on polarization characteristics. IEEE Transactions on Industrial Electronics 61(12) (2014) 6844-6851.

[11] W. F. Shun, S. X. Song, Research on Batterys charging system based on the Fuzzy control. In Proceedings of the 2nd International Conference on Computer Science and E-lectronics Engineering. 2013.

[12] J. Jiang, C. Zhang, Fundamentals and Application of Lithium-ion Batteries in Electric Drive Vehicles. John Wiley & Sons, 2015.

[13] J. B. Wang, C. Y. Chuang, A multiphase battery charger with pulse charging scheme. In 31st Annual Conference of IEEE Industrial Electronics Society, 2005, IEEE, (2005) 1248-1253.

[14] J. Jiang, C. Zhang, J. Wen, W. Zhang, S. M. Sharkh, An optimal charging method for Li-ion batteries using a fuzzy-control approach based on polarization properties. IEEE transactions on vehicular technology 62(7) (2013) 3000-3009.

[15] R. C. Cope,Y. Podrazhansky, The art of battery charging. in: Battery Conference on Applications and Advances, 1999. The Fourteenth Annual, IEEE, (1999) 233-235.

[16] L. Xu, J. Wang, Q. Chen, Kalman filtering state of charge estimation for battery management system based on a stochastic fuzzy neural network battery model. Energy Conversion and Management, 53(1) (2012) 33-39.

[17] L. Chen, R. Hsu, C. Liu, A design of a grey-predicted Li-ion battery charge system. Industrial Electronics, IEEE Transactions on, 55(10) (2008) 3692-3701.

[18] C. Li, G. Liu, Optimal fuzzy power control and management of fuel cell/battery hybrid vehicles. Journal of power sources, 192(2) (2009) 525-533.

[19] Y. Liu, J. Teng, Y. Lin, Search for an optimal rapid charging pattern for lithium-ion batteries using ant colony system algorithm. Industrial Electronics, IEEE Transactions on, 52(5) (2005) 1328-1336.

[20] X. Hu, S. Li, H. Peng, F. Sun, Charging time and loss optimization for LiNMC and LiFePO$_4$ batteries based on equivalent circuit models. Journal of Power Sources, 239 (2013) 449-457.

[21] S. Zhang, C. Zhang, R. Xiong, W. Zhou, Study on the optimal charging strategy for lithium-ion batteries used in electric vehicles. Energies, 7(10) (2014) 6783-6797.

[22] A. Abdollahi, et al. Optimal battery charging, Part I: Minimizing time-to-charge, energy loss, and temperature rise for OCV-resistance battery model, Journal of Power Sources, 303 (2016) : 388-398.

[23] R. Zhao, J. Liu, J. Gu, Simulation and experimental study on lithium ion battery short circuit. Applied Energy 173 (2016) 29-39.

[24] C. Zhang, K. Li, J. Deng, Real-time estimation of battery internal temperature based on a simplified thermoelectric model. Journal of Power Sources, 302 (2016) 146-154.

[25] R. Kroeze, P. Krein, Electrical battery model for use in dynamic electric vehicle simulations. Power Electronics Specialists Conference, IEEE ,(2008) 1336-1342.

[26] D. Domenico, A. Stefanopoulou, G. Fiengo, Lithium-ion battery state of charge and critical surface charge estimation using an electrochemical model-based extended Kalman filter. Journal of dynamic systems, measurement, and control 132(6) (2010) 061302.

[27] X. Hu, S. Li, H. Peng, A comparative study of equivalent circuit models for Li-ion batteries, Journal of Power Sources, 198 (2012) 359-367.

[28] C. Zhang, K. Li, J. Deng, S. Song, Improved Real-time State-of-Charge Estimation of LiFePO4 Battery Based on a Novel Thermoelectric Model. IEEE Transactions on Industrial Electronics.

[29] R. Rao, V. Savsani, D. Vakharia, Teaching–learning-based optimization: a novel method for constrained mechanical design optimization problems. Computer-Aided Design, 43(3) (2011) 303-315.

[30] R. Rao, Applications of TLBO Algorithm and Its Modifications to Different Engineering and Science Disciplines. In Teaching Learning Based Optimization Algorithm, Springer International Publishing (2015) 223-267.

[31] T. Dede, Application of Teaching-Learning-Based-Optimization algorithm for the discrete optimization of truss structures. KSCE Journal of Civil Engineering 18(6) (2014) 1759-1767.

[32] S. C. Satapathy, A. Naik, Modified Teaching–Learning-Based Optimization algorithm for global numerical optimization—A comparative study. Swarm and Evolutionary Computation, 16 (2014) 28-37.

[33] Z. Yang, K. Li, Q. Niu, Y. Xue, A. Foley, A self-learning TLBO based dynamic economic/environmental dispatch considering multiple plug-in electric vehicle loads. Journal of Modern Power Systems and Clean Energy, 2(4) (2014) 298-307.

[34] R. Rao, V. Savsani, D. Vakharia, Teaching–learning-based optimization: an optimization method for continuous non-linear large scale problems. Information Sciences, 183(1) (2012) 1-15.

[35] R. C. Eberhart, Y. Shi, Comparing inertia weights and constriction factors in particle swarm optimization. in Evolutionary Computation, Proceedings of the 2000 Congress on, IEEE, 1 (2000) 84-88.

Nomenclature

V battery terminal voltage
R_1, R_2 battery diffusion resistances
C_1, C_2 battery diffusion capacitances
V_1 $R_1 C_1$ network voltage
V_2 $R_2 C_2$ network voltage
U_{OCV} battery open circuit voltage
i charge current
R battery internal resistance
soc battery state of charge
C_n battery nominal capacity
T_s sampling time period
T_{in} battery internal temperature
T_{sh} battery surface temperature
T_{amb} battery ambient temperature
D_1 battery internal thermal capacity
D_2 battery surface thermal capacity
k_1, k_2 battery thermal conduction coefficients
Q battery thermal dissipation
J_{CT} battery charging time cost function
J_{EL} battery energy loss cost function
J_{TR} battery temperature rise cost function
J_{TinR} battery internal temperature rise cost function
J_{TshR} battery surface temperature rise cost function
J_{Charge} battery charging triple-objectives cost function
s_0 battery charging initial SOC
s_{tf} battery charging final SOC
i_{min} battery minimum charging current
i_{max} battery maximum charging current
V_{min} battery minimum terminal voltage
V_{max} battery maximum terminal voltage
J_{charge_CC} battery constant current process cost function
J_{charge_CV} battery constant voltage process cost function